



# Effects of vertical mixing on the Lake Michigan food web: an application of a linked end-to-end earth system model framework

H. Zhang<sup>1</sup> · D. M. Mason<sup>2</sup> · N. W. Boucher<sup>3</sup> · E. S. Rutherford<sup>2</sup> · D. J. Cannon<sup>4</sup> · J. Kessler<sup>2</sup> · A. Fujisaki-Manome<sup>4</sup> · J. Wang<sup>2</sup> · E. A. Fulton<sup>5</sup>

Received: 16 January 2023 / Accepted: 25 June 2023 / Published online: 25 July 2023  
This is a U.S. Government work and not under copyright protection in the US; foreign copyright protection may apply 2023

## Abstract

Physical processes may affect ecosystem structure and function through the accumulation, transport, and dispersal of organic and inorganic materials, nutrients, and organisms; they structure physical habitat and can influence predator–prey interactions and trophic production. In the Laurentian Great Lakes, horizontal currents generally dominate, but little is known about the effects of vertical mixing on lake food webs. We developed a linked earth system model and used it to explore how vertical mixing affects the productivity of Lake Michigan (LM), the world’s fifth-largest lake, whose food web and fisheries have been adversely affected by invasive *Dreissena* mussels. We hypothesized that higher vertical mixing would result in higher food web biomass by making phosphorus more available to the lower food web, and that filtration by invasive mussels would counter the effects of mixing and decrease food web biomass. Using linked climate, hydrodynamics, and ecosystem models, we projected the response of LM’s food web to scenarios of different levels of vertical mixing, with and without invasive mussels. Biomass of most functional food web groups increased with increases in vertical mixing, with the greatest increases in phytoplankton and zooplankton. Increased biomass was due to the replenishment of nutrients into the euphotic zone, which enhanced growth and biomass of lower trophic levels through bottom-up effects. However, filtration by invasive mussels reduced the positive effects of mixing for most species. Future applications of the linked earth system framework will explore the effects of climate warming and nutrient reduction on fisheries production to inform fisheries managers.

**Keywords** Great Lakes Earth System Model · GLESM · Finite Volume Community Ocean Model · Atlantis Ecosystem Model · Trophic production · Invasive species

## 1 Introduction

Physical processes in aquatic systems may affect ecosystem structure and function through their role in accumulation, transport, and dispersal of organic and inorganic materials,

nutrients, and organisms (Barstow 1983; Wetzel 2001; Rao and Schwab 2007; Luo et al. 2012, 2017); structuring physical habitat (Larson and Schaeztl 2001); enhancing hypoxia formation and extent (Bravo et al. 2017; Tellier et al. 2022); and influencing predator–prey interactions and trophic level production (McNaught and Hasler 1961). These physical processes occur in both the horizontal and vertical dimension and include lake circulation and vertical mixing, which in the Laurentian Great Lakes are mainly driven by winds and thermal gradients (Boyce 1974; Rao and Schwab 2007).

Relative to the effects of horizontal mixing on ecosystem processes, the effects of vertical mixing have received much less attention. Vertical mixing (often referred to as vertical turbulent diffusion—VTD) is an important physical dynamic of large and deep freshwater ecosystems that acts to deliver nutrients and organic material from the water column to the benthos, contributes to the sequestering of nutrients in the benthos, and redistributes nutrients and organic materials

---

Responsible Editor: F. Xu

---

✉ E. S. Rutherford  
Ed.Rutherford@noaa.gov

<sup>1</sup> Eureka Aquatic Research, LLC., Ann Arbor, MI, USA

<sup>2</sup> NOAA Great Lakes Environmental Research Laboratory, Ann Arbor, MI, USA

<sup>3</sup> Department of Wildlife and Fisheries, Michigan State University, East Lansing, MI, USA

<sup>4</sup> Cooperative Institute for Great Lakes Research, University of Michigan, Ann Arbor, MI, USA

<sup>5</sup> CSIRO Oceans & Atmosphere, Hobart, TAS, Australia

found on the bottom into the water column. In temperate regions, the degree and effectiveness of mixing has a seasonal dependence; during the thermally stratified seasons (summer), the exchange between surface waters and deeper depths (hypolimnion) is restricted, but during the non-stratified seasons (late fall, winter, and early spring), the thermal conditions are isothermal, the water column is well mixed, and vertical exchange is high (Wetzel 2001). The importance of these seasonal mixing patterns has been demonstrated in one- and two-dimensional water quality model studies (e.g., Boegman et al. 2008); with increased computing power, 3-dimensional models with fine spatial resolution are now prevalent (e.g., Rowe et al. 2015, 2017; Chen et al. 2002), which can emphasize both the horizontal and vertical physical processes that help to structure ecosystems.

The importance of VTD for ecosystem dynamics in the Laurentian Great Lakes is further magnified by its effects on the food web that are modified by the invasive dreissenid mussels (quagga mussel *Dreissena rostriforma bugensis*, and zebra mussel *D. polymorpha*). Dreissenid mussels are benthic filter-feeders that have altered water quality, habitat, biogeochemistry, and energy flow in four of the five Great Lakes and have negatively affected food webs and fisheries (Kerfoot et al. 2010; Vanderploeg et al. 2010; Madenjian et al. 2015; Boucher 2019). The growth of dreissenid mussels depends on the availability of organic material obtained through passive sinking from the pelagic zone, or more often, delivery through VTD to the bottom. Moreover, dreissenid mussels affect the cycling and offshore transport of phosphorus (Hecky et al. 2004). Despite phosphorus loadings to Lake Michigan remaining relatively constant, water column concentrations of nutrients have declined after quagga mussels irrupted in LM in 2004, particularly in offshore waters. Dreissenid mussel filtration acted to sequester and divert nutrients from pelagic waters to the bottom and nearshore (Hecky et al. 2004), thereby depleting nutrient concentrations available to the offshore pelagic food web. Thus, how vertical and horizontal transport processes affect dreissenid mussel filtration, growth, and food web effects are of interest to lake stakeholders, resource managers, and limnologists (Rowe et al. 2015; Shen et al. 2018, 2020) and necessitate the incorporation of VTD in a 3-dimensional ecosystem model.

Clearly, hydrodynamics plays a major role in many ecosystem processes, but they are often poorly parameterized in ecosystem models, especially those which include dynamics of an upper food web. For example, in the Atlantis Ecosystem Model (Fulton et al. 2004a, 2004b), a popular trophodynamics ecosystem model framework, VTD is largely ignored (Audzijonyte et al. 2017), yet it is an important and potentially dominant component of vertical transport materials and nutrients in large lakes and estuaries, with mixing timescales that are several orders of magnitude smaller

than those associated with advection or settling (e.g., Koseff et al. 1993). While transient wind-induced upwellings occur in many large lakes, including the Laurentian Great Lakes (e.g., Plattner et al. 2006; Rao and Schwab 2007; Li et al. 2021), VTD likely plays a more dominant role in vertical transport over large temporal and spatial scales, especially during periods of weak and no thermal stratification which can occur for up to two-thirds of the year. Thus, accurate representations of hydrodynamic processes, including seasonal mixing cycles, are imperative for meaningful ecosystem modeling and forecasting.

Herein, we evaluate the response of the Lake Michigan food web to VTD. Specifically, we focused on four VTD treatments and their influence on food web effects with and without invasive dreissenid mussels. To accomplish this, we used our Great Lakes Earth System Model (GLESIM), which is a linked model framework that uses outputs of downscaled temperature, wind, and precipitation from a climate model as external forcings for a hydrodynamics model (Great Lakes Finite Volume Community Ocean Model, GL-FVCOM), then takes the hydrodynamic output and nutrient estimates from major tributaries (Luo et al. 2017) to drive an end-to-end ecosystem model—the Lake Michigan Atlantis Model (LMAM).

## 2 Methods

### 2.1 Study ecosystem

The North American Laurentian Great Lakes (Fig. 1) are the largest freshwater system on the planet, with a total surface area of 244,160 km<sup>2</sup>, and contain about 21% of the world's surface freshwater and about 84% of North America's surface freshwater ([https://ijc.org/sites/default/files/SAB\\_Great-Lakes-Science-Strategy-summary-report\\_2022.pdf](https://ijc.org/sites/default/files/SAB_Great-Lakes-Science-Strategy-summary-report_2022.pdf) accessed on 1/3/2023). The lakes also provide valuable ecosystem services to over 38 million people residing in the basin. The lakes provide drinking water and support agriculture, transportation, commercial shipping, hydroelectric power, and a wide variety of recreational opportunities including a world-class fishery that generates approximately \$7 billion USD per year (Krantzberg and De Boer 2008). Of the five Great Lakes, Lake Michigan is the second largest Great Lake by volume (4918 km<sup>3</sup>), the third largest by area (57,763 km<sup>2</sup>), and is also the fifth largest lake (by area, 6th by volume) in the world (<https://www.glc.org/lakes/lake-michigan>, accessed 12/21/2022). As with many large ecosystems, Lake Michigan has, and continues to experience, many human-induced stressors including climate change, invasive species, and high nutrient concentrations in coastal waters that contribute to harmful algal blooms (HABs) and hypoxia (Vanderploeg et al. 2002; Tomlinson et al. 2010; Allan et al.

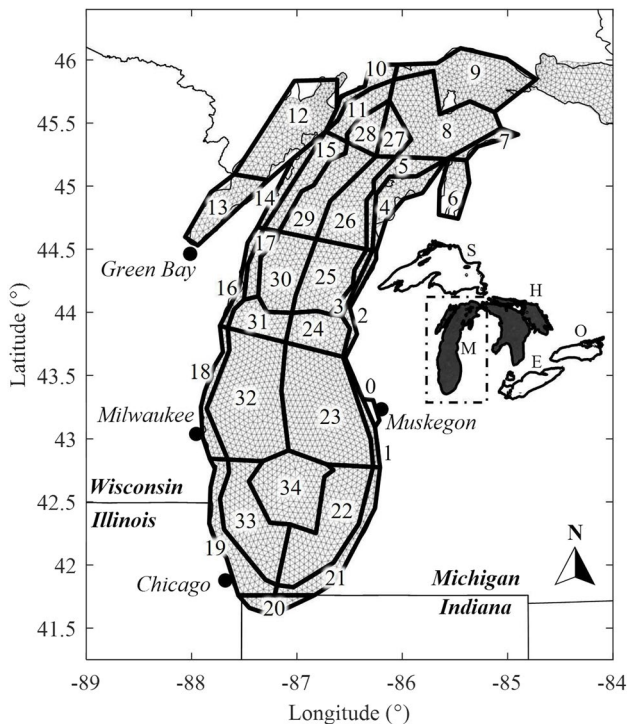


**Fig. 1** Map of the Lake Michigan Atlantis model spatial domain. Atlantis polygons (thick lines) are numbered individually, and the unstructured triangular grid cells (thin lines) used for GL-FVCOM are included for reference. An inset diagram is included to show the full GL-FVCOM model domain (Lake Michigan-Huron) in relation to all five Laurentian Great Lakes (S: Superior, H: Huron, M: Michigan, E: Erie, and O: Ontario). GL-FVCOM simulated water temperatures are rescaled to the average for each polygon and depth stratum, while fluxes (vertical and horizontal) are the average flux (direction and magnitude) across each polygon/stratum segment

2013; Klump et al. 2018; Miller et al. 2022), but low nutrient concentrations in the offshore area.

## 2.2 Great Lakes Earth System Model (GLESM): linked model framework overview

GLESM integrates and links climate, weather, watersheds, hydrodynamics, and chemical and food web processes into a modeling framework that provides capabilities for hindcasts, nowcasts, and forecasts of regional effects (natural and anthropogenic) on the Laurentian Great Lakes. Here, we highlight GLESM’s capabilities through weather-forced circulation and mixing on the food web of the Laurentian Great Lakes.

### 2.2.1 Hydrodynamics

Lake Michigan’s physics and thermodynamics were simulated using the Great Lakes Finite Volume Community Ocean Model (GL-FVCOM), a spherical-coordinate,

unstructured-grid hydrodynamic model designed to solve the primitive (i.e., hydrostatic) equations. GL-FVCOM was originally implemented by Bai et al. (2013), who modified the original FVCOM initially developed by Chen et al. (2003, 2006, 2013). GL-FVCOM incorporates several modifications to the original FVCOM scripts (version 3.1.6), including the use of the internal ice module (Gao et al. 2011) based on a coupled elastic-viscous-plastic rheology ice model (CICE: Hunke and Dukowicz 1997) and a wind-wave mixing boundary condition scheme developed by Hu and Wang (2010). Both modifications dramatically improved modeled surface temperature and subsurface thermal structure in the Laurentian Great Lakes, which are particularly important for ecological modeling. The horizontal computational grid is composed of unstructured triangular elements, and vertical layers are delineated using a terrain-following  $\sigma$ -coordinate scheme with increased resolution at the surface and bottom boundaries. Additional details on model parameterization can be found in Cannon et al. (2023) and Wang et al. (2023).

For this study, the GL-FVCOM model domain included both Lake Michigan and Lake Huron, which are connected through the Straits of Mackinac and share a common water elevation (Fig. 1). Although the lakes are often discussed and managed separately, their hydrologic connection requires combined modeling for accurate hydrodynamic simulations. For simplicity, the lakes were modeled as an enclosed basin, and all mass fluxes (i.e., inflows, outflows, evaporation, precipitation) were ignored. The horizontal resolution of the model grid ranged from 3 to 5 km, with 21 vertical sigma levels used for subsurface computations. Model results for each lake were separated during post-processing, and only model grid cells in Lake Michigan were retained for further analysis. Model outputs, including vertical and lateral advective exchange rates and water column temperatures, were rescaled and averaged over larger sub-domains and depth layers (see Supplementary Information) for input into the Atlantis Ecosystem Model (discussed below: 34 boxes; maximum 6 layers per box).

### 2.2.2 Ecosystem model

Lake Michigan Atlantis Model (LMAM) was developed and integrates physical, chemical, ecological, and fisheries dynamics in a three-dimensional, spatially explicit framework. The framework was initially developed by Fulton et al. (Fulton 2001; Fulton et al. 2003, 2004a, 2004b, 2004c) that includes a 3-dimensional rendering of an ecosystem and five modules: hydrographic, ecology, and three management and human use modules (harvest sub-model, assessment sub-model, and economics sub-model). Here, we only focus on the two core modules: hydrographic and ecology modules.

The hydrographic module in LMAM accepts inputs (i.e., water temperature, vertical and horizontal fluxes) from the

rescaled output of GL-FVCOM, which are used as forcing functions in the ecological module. In the ecological module, nutrient dynamics, organismal growth, mortality, consumption, recruitment, physical transport/behavioral movement, and habitat dependency are modeled in each polygon as a system of differential equations on a 12-h time step. Primary producers and invertebrates are represented as biomass pools and vertebrates as age-structured populations (Table 1).

Here, our emphasis is on vertical mixing and its effects on the food web. Thus, modifications to vertical mixing were done in the hydrographic module of Atlantis and not in GL-FVCOM. Atlantis includes a simple diffusion function designed to simulate mixing throughout the water column using a constant turbulent vertical diffusion coefficient ( $K_z$ ), which is often set to molecular or near-molecular diffusion levels ( $1 \times 10^{-7} - 10^{-6} \text{ m}^2/\text{s}$ ). These

weak mixing coefficients are unrealistic in Lake Michigan, where vertically averaged hypolimnetic mixing rates have been observed to vary between  $1 \times 10^{-5}$  and  $10^{-2} \text{ m}^2/\text{s}$  over the seasonal stratification cycle (Cannon et al. 2021). To explore this assumption of weak vertical mixing, we designed four parameterized mixing treatments: (1) three levels of annual average constant VTD ( $K_z = 1 \times 10^{-5}$ ,  $10^{-4}$ ,  $10^{-3} \text{ m}^2/\text{s}$ ; hereafter referred to as C5, C4, and C3, respectively); and (2) a sinusoidally varying seasonal VTD (hereafter referred to as S, with an annual average of  $1 \times 10^{-3.85} \text{ m}^2/\text{s}$ ) (Table 2, Fig. 2). The S scenario was designed to mimic the modeled (and observed) seasonal cycle of mixing in Lake Michigan (Fig. 2), with depth-averaged turbulent diffusion rates that varied between  $1 \times 10^{-5} \text{ m}^2/\text{s}$  in the summer and  $1 \times 10^{-2} \text{ m}^2/\text{s}$  in the winter. S coefficients ( $K_{z\text{-seasonal}}$ ) were explicitly defined based on the day of year (doy, range: 1–366), such that

**Table 1** List of model groups in the Lake Michigan Atlantis Model. Model groups are categorized as “functional groups,” including piscivorous fish (PISC), omnivorous fish (OMNI), planktivorous fish (PLAN), benthivorous fish (BENV), benthic invertebrates (BENT), zooplankton (ZOO), macro-algae (MACR), phytoplankton (PHYTO), microbes (MICR), detritus (DETR). Initial biomass ( $\text{MT}/\text{km}^2$ ) is the basin wide average biomass at the start of the model simulation based on a Lake Michigan Ecopath model (Rutherford et al. 2021). “Modeled as” refers to whether the model group was modeled as an age-structured population or as a biomass pool

Long name	Functional group	Scientific names	Initial biomass	Modeled as
Chinook salmon	PISC	<i>Oncorhynchus tshawytscha</i>	0.126	Age-structured
Coho salmon	PISC	<i>Oncorhynchus kisutch</i>	0.018	Age-structured
Steelhead trout	PISC	<i>Oncorhynchus mykiss</i>	0.112	Age-structured
Lake trout	PISC	<i>Salvelinus namaycush</i>	0.094	Age-structured
Burbot	PISC	<i>Lota lota</i>	0.317	Age-structured
Walleye	PISC	<i>Sander vitreus</i>	0.013	Age-structured
Yellow perch	OMNI	<i>Perca flavescens</i>	0.045	Age-structured
Lake whitefish	OMNI	<i>Coregonus clupeaformis</i>	0.457	Age-structured
Alewife	PLAN	<i>Alosa pseudoharengus</i>	2.468	Age-structured
Bloater	PLAN	<i>Coregonus hoyi</i>	3.956	Age-structured
Rainbow smelt	PLAN	<i>Osmerus mordax</i>	1.026	Age-structured
Slimy sculpin	BENV	<i>Cottus cognatus</i>	0.167	Age-structured
Deepwater sculpin	BENV	<i>Myoxocephalus thompsonii</i>	0.733	Age-structured
Round goby	BENV	<i>Neogobius melanostomus</i>	0.010	Age-structured
Dreissenid mussels	BENT		1.040	Biomass pool
Amphipods	BENT		0.816	Biomass pool
Chironomids	BENT		0.644	Biomass pool
Diporeia	BENT		16.940	Biomass pool
Oligochaetes	BENT		10.146	Biomass pool
Mysis	ZOOP		2.837	Biomass pool
Bythotrephes	ZOOP	<i>Bythotrephes longimanus</i>	0.172	Biomass pool
Copepods	ZOOP		26.106	Biomass pool
Cladocerans	ZOOP		5.748	Biomass pool
Rotifers	ZOOP		1.166	Biomass pool
Macroalgae	MACR		0.090	Biomass pool
Nanoplankton ( $> 2 \mu\text{m}$ )	PHYT		4.389	Biomass pool
Picoplankton ( $< 2 \mu\text{m}$ )	PHYT		3.526	Biomass pool
Protozoa	MICR		2.258	Biomass pool
Pelagic bacteria	MICR		32.974	Biomass pool
Benthic bacteria	MICR		13.350	Biomass pool
Labile detritus	DETR		5.403	Biomass pool
Refractory detritus	DETR		5.403	Biomass pool

**Table 2** Description of Atlantis model scenario simulations. The model used for calibration is shown with (\*)

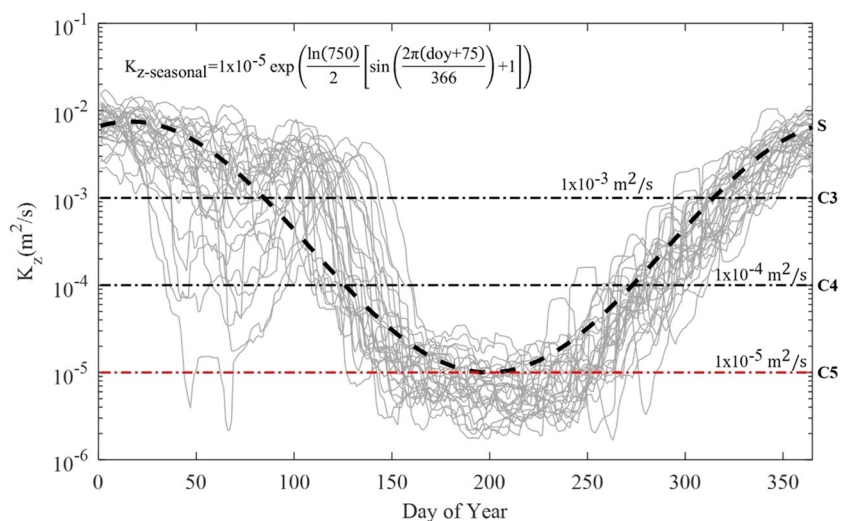
Scenarios	Treatments
S_M*	Sinusoidal seasonal vertical mixing, mussels
S_noM	Sinusoidal seasonal vertical mixing, no mussels
C5_M	Constant vertical mixing ( $K_z = 1 \times 10^{-5} \text{ m}^2/\text{s}$ ), mussels
C5_noM	Constant vertical mixing ( $K_z = 1 \times 10^{-5} \text{ m}^2/\text{s}$ ), no mussels
C4_M	Constant vertical mixing ( $K_z = 1 \times 10^{-4} \text{ m}^2/\text{s}$ ) mussels
C4_noM	Constant vertical mixing ( $K_z = 1 \times 10^{-4} \text{ m}^2/\text{s}$ ), no mussels
C3_M	Constant vertical mixing ( $K_z = 1 \times 10^{-3} \text{ m}^2/\text{s}$ ), mussels
C3_noM	Constant vertical mixing ( $K_z = 1 \times 10^{-3} \text{ m}^2/\text{s}$ ), no mussels

$$K_{z\text{-seasonal}} = 10^{-5} \exp\left(\frac{\ln(750)}{2} \left[\sin\left(\frac{2\pi(\text{doy} + 75)}{366}\right) + 1\right]\right) \quad (1)$$

For each mixing scenario, VTD coefficients in Atlantis were set equal to  $K_z = 1 \times 10^{-5}, 10^{-4}, 10^{-3} \text{ m}^2/\text{s}$  or  $K_{z\text{-seasonal}}$  at all depth layers in offshore model boxes (i.e., boxes not touching the coast). For all scenarios, nearshore (i.e., boxes along the coast) VTD coefficients were increased by an order of magnitude to simulate the turbulence-enhancing effects of coastal boundary layers.

We recognize that because the seasonal VTD coefficient described here is not directly linked to hydrodynamic forcing inputs (i.e., lake temperatures, current velocities), the day-to-day lake physics may be dynamically inconsistent. For example, there may be days where parameterized mixing rates are high, despite the presence of turbulence-limiting thermal stratification in a given model box. However, given the relatively consistent annual cycle of lake-wide vertical mixing rates (e.g., Fig. 2), we expect the effects of dynamic inconsistencies to be relatively minor, especially when integrated over the large spatial and temporal scales discussed in this manuscript.

**Fig. 2** Time series of lake-averaged vertical turbulent scalar diffusivity (VTD) where  $K_z$  is constant turbulent vertical diffusion coefficient at near-molecular diffusion levels. Light gray lines are outputs from the GL-FVCOM from 1994 to 2021, and the dashed black and red lines are the VTD functions used in the Atlantis Ecosystem Model simulations. The S parameterization was for seasonally varying VTD, while C3–C5 were constant VTD parameterizations. The C5 VTD (red) was the baseline for comparison of VTD effects



### 2.3 LMAM configuration and calibration

The spatial domain for LMAM was designed to balance spatial resolution relative to optimizing computer runtime (in a Windows-based system). Model polygons were defined based on lake bathymetry (nearshore is depths less than 30 m; offshore is depths between 30 and 110 m; deep offshore is depths greater than 110 m), tributary inputs, state boundaries, and pre-existing fishery management statistical districts (Madenjian 2019). Nutrients were added to the nearshore polygons to represent major sources of nutrient loading into the lake. The final spatial domain included 34 active polygons and one boundary box located at Muskegon Lake (Fig. 1), and up to 6 water depth layers (also see Supplementary Information). The dynamics of 30 organismal groups were simulated, including 14 fish groups, 5 zooplankton groups, 5 benthic groups, 3 microbial groups, 2 phytoplankton groups, and one macroalga group (Table 1). In addition, there were three non-living groups which included two detritus groups and one carrion group. Nutrients (nitrogen and phosphorus) were dynamically simulated (see Supplementary Information for more details).

The model was initialized using observed values from 1994 to 1998 and was driven by forcings of fishery catch (1994–2013), nutrient loads (1994–2008), fish stocking (1994–2013), and hydrodynamics (1994–2021) including the simulation (and observation) based sinusoidally varying seasonal VTD mixing in Lake Michigan (Fig. 2). Nutrient loads after 2008 were set to the average of 2004–2008 loadings. Fishery catch and fish stocking after 2013 were set to the observed values from 2013. We compared the simulated population biomass (MT/km²) of dreissenids and other selected model groups/species of interest to observed data. We calibrated the model by comparing simulated population biomass to

lake-averaged biomass of 21 model groups or species. We focused on the calibration of phytoplankton, the base of the food web, and on upper trophic levels, especially alewife, chinook salmon, coho salmon, and lake trout. These groups are key drivers of Lake Michigan's economically valuable recreational fisheries and a current focus of fisheries managers and contain the most complete time series data.

## 2.4 Scenario simulations and analysis

We used LMAM to run eight scenario simulations to understand how VTD may affect the food web biomass, with and without the presence of invasive mussels in the food web (Table 2). Specifically, the scenarios included eight full combinations of two mussel treatments (with mussels and without mussels) and four VTD treatments, and each scenario was run with a 12-h time step for 100 simulation years. We compared the model output of the vertical distribution of SRP and nanoplankton in a deep offshore habitat, box 23 (Fig. 1) during winter and summer. We also calculated the total phosphorus in the water column of box 23 and in the euphotic zone (to 40 m) for each scenario during winter and summer. Furthermore, we aggregated the biomass of model species or groups within similar trophic levels together into 9 functional groups, including piscivorous fish, omnivorous fish, planktivorous fish, benthivorous fish, benthic invertebrates, zooplankton, macroalgae, phytoplankton, and microbes (Table 1). For reporting purposes, simulated biomasses of functional groups were averaged across horizontal polygons and depths for the whole lake (MT/km<sup>2</sup>) and summarized as average biomass for the last 20 years (years 80–100) of the simulation. The biomass response of functional groups to the VTD mixing scenarios was compared to functional group biomass response to the corresponding lowest VTD mixing scenarios (C5\_M or C5\_noM as baselines) and was reported as the relative percent change as follows, using seasonally varying mixing with mussels S\_M as an example):

$$\frac{S\_M \text{ biomass} - C5\_M \text{ biomass}}{C5\_M \text{ biomass}} \times 100 \quad (2)$$

We considered biomass changes of functional groups relative to the corresponding baseline C5 scenarios (C5\_M and C5\_noM) as strong effects if their absolute values were  $\geq 20\%$ , as intermediate effects if absolute change values were from 10 to 19%, and as negligible effects if absolute change values were  $< 10\%$ .

## 3 Results

### 3.1 Model calibrations to data (GL-FVCOM, Atlantis)

GL-FVCOM simulated forcing data were validated against observations in Lake Michigan. Lake-averaged ice cover and lake surface temperatures were compared to remote sensing observations available through the Great Lakes Surface Environmental Analysis (<https://coastwatch.glerl.noaa.gov>). Ice cover estimates were generally within 10% of observations, and mean lake surface temperature biases were less than 0.75 °C, with a root mean square error of 1 °C in Lake Michigan. Modeled temperature structure and stratification were compared to in situ mooring observations in each lake (NOAA GLERL 2019a, 2019b). Modeled temperature structure highlighted overly diffuse thermoclines during the stratified period, with maximum root mean square errors of  $\sim 3$  °C at 30 m depth. These biases are not expected to have a detrimental impact on ecological simulations, especially considering the relatively low vertical resolution of the ecological model (6 layers) compared to the hydrodynamic model (21 layers). Simulated seasonal surface current patterns (Figure SI-1) also compared favorably with previous observational (Beletsky et al. 1999) and modeling (e.g., Beletsky and Schwab 2008) studies, with increased coastal current speeds and counter-clockwise gyres in the north and south basins. Additional details on model validation can be found in Cannon et al. (2023).

Atlantis model calibration was performed for 21 food web groups (Figures SI-6, SI-7; Table SI-7). Simulated biomass of most model groups agreed well with the trends and/or magnitudes of biomass measured from field surveys, including Nanoplankton, *Mysis*, *Diporeia*, *Dreissena*, Alewife *Alosa pseudoharengus*, Bloater *Coregonus hoyi*, Rainbow Smelt *Osmerus mordax*, Deepwater Sculpin *Myoxocephalus thompsonii*, Simy Sculpin *Cottus cognatus*, Round Goby *Neogobius melanostomus*, Lake Whitefish *Coregonus clupeaformis*, Burbot *Lota lota*, Lake Trout *Salvelinus namaycush*, and Coho Salmon *Oncorhynchus kisutch*. Simulated biomass was higher than observed values and did not match the temporal trend in the observed values (if there were trends) for rotifers, herbivorous cladocerans, *Bythotrephes longimanus* (invasive predacious Cladocera), oligochaetes, Steelhead *O. mykiss*, and Chinook Salmon *O. tshawytscha*. The discrepancy between observed and modeled biomass of chinook salmon in later years reflected a cut in stocking after 2013 that was not included in the model.

### 3.2 VTD effects on vertical distribution of nutrients and nanoplankton

Nutrients and plankton showed different vertical distributions under VTD scenarios (Fig. 3). Phosphorus is often

the limiting nutrient in freshwater, so we present a vertical distribution of soluble reactive phosphorus (SRP) in a representative offshore model box (box 23, located in southeast Lake Michigan). For scenarios of C5\_M, C4\_M, C3\_M, and S\_M, SRP concentrations during summer were low in the upper water column and high in the lower water column, with a very low SRP concentration at the surface. SRP concentration in the upper water column was the highest under the C3\_M scenario. During winter, SRP concentration increased in the water column compared to summer and was distributed almost homogeneously in the water column under S\_M and C3\_M. However, for C5\_M and C4\_M during the winter, SRP showed a similar pattern as the summer, lower in the upper water column and higher in the lower water column. Nanoplankton biomass exhibited a different seasonal vertical distribution than did SRP. During summer, nanoplankton biomass was high in the upper water column and low in the lower water column under the scenarios of S\_M and C3\_M, but was consistently low throughout the water column under the scenarios of C5\_M and C4\_M. During winter, nanoplankton biomass was homogenous and low throughout the water column under all four mixing scenarios.

The total phosphorus (TP) content in the water column (SRP plus phosphorus from organic sources including organismal biomass) increased with increased levels of constant mixing (from low C5\_M to high at C3\_M), while S\_M had a similar water column TP concentration as under C4\_M for

summer and winter. TP concentration in the water column was similar or slightly higher during summer than during winter for each scenario (Table 3). TP concentration in the euphotic zone (< 40 m) also increased with increased levels of constant mixing and was relatively stable between summer and winter across scenarios.

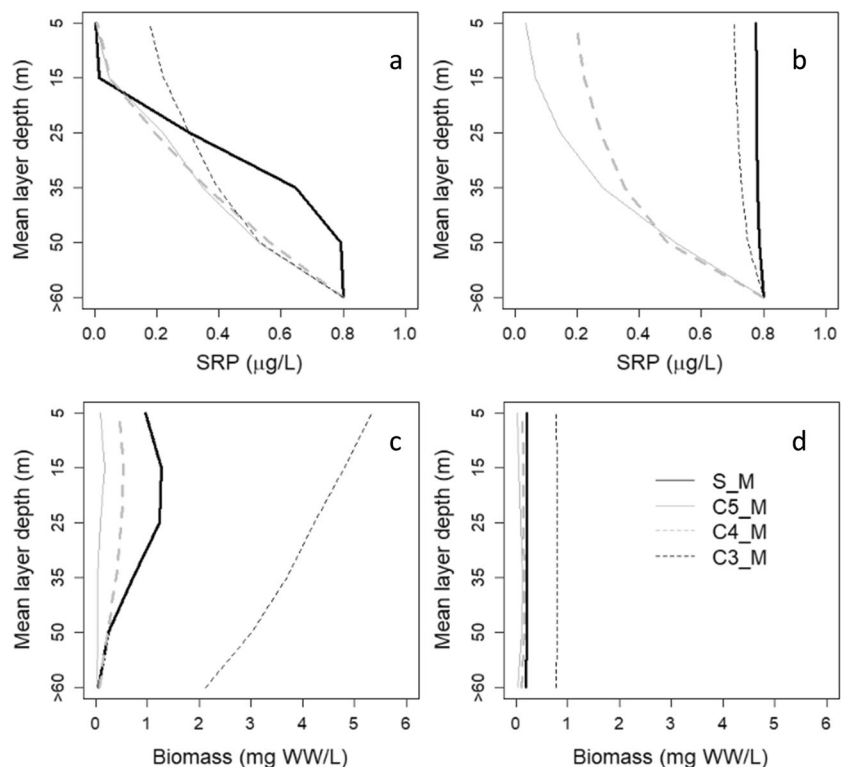
### 3.3 VTD effects on the Lake Michigan food web with invasive mussels

Under the treatments with invasive mussels, compared to the low constant mixing scenario (C5\_M), the total biomass of the whole food web increased by 24, 42%, and 541% with increasing levels of mixing (under 4C\_M, S\_M, and 3C\_M, respectively) (Table 4). When functional food web groups were considered, the C4\_M mixing scenario had large positive effects ( $\geq 20\%$  above the baseline C5\_M biomass) on the

**Table 3** Total phosphorus (MT/km<sup>2</sup>) in the water column and euphotic zones under different scenarios

Scenarios	Water column		Euphotic zone	
	Summer	Winter	Summer	Winter
C5_M	0.38	0.37	0.02	0.02
C4_M	0.52	0.50	0.07	0.04
C3_M	1.51	1.37	0.72	0.84
S_M	0.52	0.49	0.09	0.07

**Fig. 3** Vertical distribution of simulated soluble reactive phosphorus (SRP, upper panel) and nanoplankton biomass (lower panel) for 2020 summer (left panels) and winter (right panels) under scenarios of S\_M, 5C\_M, 4C\_M, and 3C\_M in an offshore box 23 (see Fig. 1 for box ID)



biomass of omnivorous fish, zooplankton, macroalgae, and phytoplankton, increasing by 85, 64, 26, and 61%, respectively, and had intermediate positive effects (10–19% above C5\_M biomass) on piscivorous fish biomass by 11%, but had negligible changes (between –10% and +10% change from C5\_M biomass) on planktivorous fish, benthivorous fish, benthos, and microbes. The S\_M mixing scenario had similar positive effects on the functional groups as C4\_M, except that S\_M increased microbe biomass by 20%. Both C4\_M and S\_M showed negligible negative effects on benthivorous fish and benthos. The highest mixing scenario (C3\_M) had large positive effects on all functional groups, except on benthivorous fish which increased by 11% above baseline.

### 3.4 VTD effects on the food web without dreissenid mussels

Under the no-mussel treatment, compared to baseline C5\_noM, the total biomass of the food web under the C4\_noM, S\_noM, and C3\_noM scenarios increased by 85, 97, and 734%, respectively (Table 4). For the aggregated trophic groups, C4\_noM, S\_noM, and C3\_noM had large positive effects on almost all functional groups, except that C4\_noM had negligible effects on planktivorous fish and benthos, and S\_M had intermediate positive effects on planktivorous fish and benthos. Compared to other no-mussel scenarios, the

C3\_noM scenario had the largest positive effects on each functional group.

### 3.5 Food web effects of VTD between scenarios of invasive mussels and no mussels

Relative to the baseline C5 scenarios, higher mixing scenarios increased the total biomass of the food web more under the no-mussel treatment compared to a treatment with mussels in the food web (85% vs 24%, 97% vs 42%, and 734% vs 542% for C4, S, and C3, respectively). For all functional groups, percent changes in biomass were higher for the scenario of no invasive mussels in the food web compared to one with invasive mussels in the food web (Table 4). Moreover, C4 and S mixing scenarios with mussels had slightly negative effects (although negligible) on benthivorous fish and benthos, but had positive effects (up to 62% increase in biomass) under the scenario of no invasive mussels.

## 4 Discussion

Our scenario simulations indicated that VTD mixing had an overall positive effect on most food web groups, with some exceptions. VTD acted to replenish nutrients in the euphotic zone which stimulated production up the food web from phytoplankton to microbes, then to zooplankton and

**Table 4** Model output for functional groups with respect to each mixing scenario. See Table 2 for mixing scenario (column header) definitions. Species/group-specific changes in response to S\_M and C5\_M can be found in the Supplementary Information (Figure SI-8)

Group	C5_M	C5_noM	C4_M	C4_noM	C3_M	C3_noM	S_M	S_noM
Percent change in biomass								
Piscivore			10.7	36.4	346.0	1098.2	13.2	53.3
Omnivore			85.2	61.1	260.6	190.7	36.0	50.7
Planktivore			1.1	8.7	62.6	191.8	2.6	14.1
Benthivore			-4.3	62.2	10.8	249.6	-0.5	61.4
Benthos			-8.8	3.8	103.7	239.8	-5.2	17.4
Zooplankton			64.4	70.8	1330.2	1155.0	55.5	87.0
Macroalgae			26.1	201.2	33.1	118.4	18.4	165.5
Phytoplankton			60.8	73.3	2648.6	2263.8	165.1	202.3
Microbe			8.5	103.9	243.0	343.7	19.9	79.9
Total			23.7	85.3	541.5	734.2	41.6	96.5
Biomass								
Piscivore	5.0	5.7	5.5	7.8	22.3	68.2	5.6	8.7
Omnivore	7.6	12.4	14.0	20.0	27.3	36.1	10.3	18.7
Planktivore	25.4	26.8	25.7	29.1	41.4	78.1	26.1	30.5
Benthivore	10.8	6.5	10.3	10.6	12.0	22.8	10.7	10.5
Benthos	158.7	172.6	144.7	179.1	323.2	586.5	150.4	202.5
Zooplankton	149.7	202.9	246.1	346.5	2140.9	2546.9	232.7	379.6
Macroalgae	125.6	107.6	158.3	324.1	167.1	234.9	148.6	285.6
Phytoplankton	155.4	189.0	249.9	327.6	4271.5	4468.0	412.0	571.4
Microbe	431.5	513.6	468.3	1047.3	1480.0	2279.1	517.5	923.8
Total	1069.6	1237.1	1322.9	2292.0	8485.7	10,320.6	1514.1	2431.4



their invertebrate and vertebrate predators, and ultimately to piscivores. Differences in magnitude and direction of organism biomass response to VTD were also driven by invasive mussel filtration of phytoplankton and alteration of nutrient cycling, and predator prey interactions which acted to dampen the biomass response of some species or groups to VTD.

Effects of VTD mixing generally were greater for lower trophic levels than for higher trophic levels and greater for pelagic organisms than for benthic organisms. Most benthic invertebrates and their predators, benthivorous fish had a negligible response to low VTD scenarios. The pelagic food web response to VTD was higher for phytoplankton and zooplankton than for planktivorous fish and their predators, piscivorous fish (Leonhardt et al. 2020). The difference between upper and lower trophic levels in their response to VTD and mussels is consistent with observations by McMeans et al. (2016) who suggested that the generalized feeding strategies and movements of large, higher trophic taxa can lead to a food web structure that is adaptive in its response to environmental changes such as variability in production or effects of invasive species.

Several studies have documented negative effects of invasive mussels on food web biomass and trophic transfer efficiency (Bunnell et al. 2018; Trumpinkas et al. 2022). Our model results suggest that ecosystem biomass may be further suppressed under a climate warming scenario, which would weaken VTD by increasing the duration of thermal stratification and shift the lake from a dimictic condition to a more monomictic condition. Rowe et al. (2017) modeled the relative influence of climate warming, nutrients, and invasive mussels on the Lake Michigan lower food web and found that the influence of *Dreissena* mussels on plankton was reduced during thermal stratification. Their model suggested warmer weather would deepen mixing of the water column, thereby reducing nutrient flux and increasing mussel filtration in the nearshore but lower mussel filtration offshore.

To build a framework of complex models to address critical issues of environmental change, we made assumptions and accepted variance in model tuning that we plan to address in future applications. The Atlantis model calibration was satisfactory for many but not all food web species or groups. For example, we may have underestimated the effects of invasive mussels on the food web response to VTD. The LMAM coupled framework was able to project the relative influence of VTD on invasive mussel cycling of phosphorus and reduction in biomass of phytoplankton caused by dresenids grazing in Lake Michigan food web, which has been well documented for the Great Lakes food webs (Hecky et al. 2004; Fahnenstiel et al. 2010; Vanderploeg et al. 2015; Pothoven and Vanderploeg 2020). However, not included in our simulations were consequences of the indirect effects of mussels on

light, the vulnerability of prey to predators, consequent behavioral responses and interactions (Bourdeau et al. 2015), or the increased importance of mussel veligers to plankton, larval fish diets, and fish recruitment in the food web (Epehimer et al. 2019).

Our study demonstrated the effects of vertical mixing on the Lake Michigan food web could be similar between using a model/observation-based sinusoidally varying seasonal VTD or an annual averaged constant VTD. Using an annual averaged constant VTD may be reasonable for investigating annual phenomena, but a model/observation-based sinusoidally varying seasonal VTD has its advantages in projecting seasonal phenomena or those of finer temporal scales, and these seasonal measures can provide the means to help refine the GL-FVCOM model for determining longer-term phenomena associated with climate change. Moreover, seasonal varying VTD is how a temperate lake operates. In the Great Lakes, VTD varies seasonally (e.g., Cannon et al. 2021) with limited diffusion rates ( $K_z = 1 \times 10^{-5} \text{ m}^2/\text{s}$ ) during the thermally stratified summer months and with energetic and full water column mixing rates ( $K_z = 1 \times 10^{-4} - 10^{-2} \text{ m}^2/\text{s}$ ) during the fall-winter-early spring isothermal months.

We also exaggerated the difference among mixing treatments in the nearshore zone. When lakes are covered by ice, there should be less mixing in winter, but still full water column mixing in the spring and fall. Ice cover can drastically reduce vertical mixing during winter, blocking wind forcing and generating turbulence-suppressing inverse stratification in the surface mixed layer. As well, there have been few observations of Great Lakes ecosystems taken under the ice, and there are virtually no data on how the Great Lakes ecosystems respond to vertical mixing under winter conditions (Wang et al. 2012; Ozerisky et al. 2021). In future, we plan to examine the effects of reduced ice cover on vertical mixing to understand how that may affect fish species recruitment and food web productivity.

Although it was beyond the scope of the present study, which focused on testing the effects of improved turbulence parameterizations, in the future, we plan to modify the LMAM to accept time series of vertically variable turbulent diffusion coefficients as forcing inputs from more observations or from hydrodynamics outputs. While assumptions of depth-uniform vertical turbulent diffusion coefficients are reasonable for the energetic fall and winter, the vertical structure of VTD is heavily influenced by water density stratification during the summer, when mixing rates outside the surface and bottom boundary layers fall to near-molecular levels (i.e.,  $K_z \approx 10^{-7} \text{ m}^2/\text{s}$ ; Cannon et al. 2021). This weak hypolimnetic mixing acts as a barrier to benthic particle delivery, reducing the effective filtration rate of mussels in deeper waters (Shen et al. 2018; Rowe et al. 2017).

## 5 Conclusions

1. We used linked climate, hydrodynamics, and ecosystem models to project the response of LM's food web to seasonally variable and seasonally constant vertical mixing scenarios, with and without invasive mussels.
2. Relative to constant low vertical mixing, seasonally varying vertical mixing increased biomass of the total food web biomass by 42% and of most food web groups by replenishing nutrients in the euphotic zone, which enhanced phytoplankton growth and biomass of lower trophic levels through bottom-up effects. High levels of constant vertical mixing acted to further increase the biomass of most food groups.
3. Without invasive mussels in the food web, all scenarios of vertical mixing acted to increase the biomass of the total food web biomass. Filtration by invasive mussels reduced the positive effects of seasonally varying mixing on most species.
4. A constant vertical mixing scenarios of  $K_z = 1 \times 10^{-4} \text{ m}^2/\text{s}$  provided similar food web effects as the seasonally variable mixing scenario. However, (a) seasonally varying vertical mixing best represents what actually occurs in nature (Cannon et al. 2021), and it can be captured in hydrodynamic models, and (b) the ability of a single constant vertical mixing coefficient may vary annually, and the ability of the model to capture future conditions under climate change cannot be assumed. Therefore, we recommend using seasonal varying vertical mixing to best capture current and future food web response to seasonal and annual changes in lake hydrodynamics, water temperature, precipitation, and ice cover resulting from climate change.

**Supplementary Information** The online version contains supplementary material available at <https://doi.org/10.1007/s10236-023-01564-w>.

**Acknowledgements** We appreciate financial support for the Great Lakes Earth System Model project from the National Oceanic Atmospheric Administration (NOAA) Office of Oceanic and Atmospheric Research (OAR) Ocean Sciences Portfolio, NOAA Great Lakes Environmental Research Laboratory (GLERL), the Great Lakes Fishery Commission (GLFC), and the United States (US) Environmental Protection Agency (EPA) Great Lakes Restoration Initiative. Long-term monitoring and research data used to construct the Lake Michigan Atlantis model were provided in part by several agencies, including NOAA GLERL, U.S. EPA's Great Lakes National Program Office's Monitoring Program, Great Lakes Fishery Commission's Great Lakes Databases, United States Geological Survey Great Lakes Science Center's trawl and hydroacoustics surveys, and piscivore abundance data from statistical catch-at-age models developed and run by Michigan State University's Quantitative Fisheries Center. We thank S. Gibson for assistance with data compilation, and L. Mason for developing the vertical and horizontal grids for the Lake Michigan Atlantis model.

**Data availability** All data generated or analyzed for this study are available from the corresponding author on reasonable request.

## Declarations

**Conflict of interest** The authors declare no competing interests.

**Open Access** This article is licensed under a Creative Commons Attribution 4.0 International License, which permits use, sharing, adaptation, distribution and reproduction in any medium or format, as long as you give appropriate credit to the original author(s) and the source, provide a link to the Creative Commons licence, and indicate if changes were made. The images or other third party material in this article are included in the article's Creative Commons licence, unless indicated otherwise in a credit line to the material. If material is not included in the article's Creative Commons licence and your intended use is not permitted by statutory regulation or exceeds the permitted use, you will need to obtain permission directly from the copyright holder. To view a copy of this licence, visit <http://creativecommons.org/licenses/by/4.0/>.

## References

- Allan JD, McIntyre PB, Smith SDP, Halpern BS, Boyer GL, Buchsbaum A et al (2013) Joint analysis of stressors and ecosystem services to enhance restoration effectiveness. *Proc Natl Acad Sci* 110:372–377
- Audzijonyte A, Gorton R, Kaplan I, Fulton EA (2017) Atlantis user's guide part I: General overview, physics & ecology. CSIRO, Hobart, Australia
- Bai X, Wang J, Schwab DJ, Yang Y, Luo L, Leshkevich GA, Liu S (2013) Modeling 1993–2008 climatology of seasonal general circulation and thermal structure in the Great Lakes using FVCOM. *Ocean Model*. <https://doi.org/10.1016/j.ocemod.2013.02.003>
- Barstow SF (1983) The ecology of Langmuir circulation: a review. *Mar Environ Res* 9:211–236
- Beletsky D, Schwab D (2008) Climatological circulation in Lake Michigan. *Geophys Res Lett* 35:L21604. <https://doi.org/10.1029/2008GL035773>
- Beletsky D, Saylor JH, Schwab DJ (1999) Mean circulation in the Great Lakes. *J Great Lakes Res* 25(1):78–93
- Boegman L, Loewen MR, Hamblin PF, Culver DA (2008) Vertical mixing and weak stratification over zebra mussel colonies in western Lake Erie. *Limnol Oceanogr* 53:1093–1110
- Boucher N (2019) Examining the relative effects of nutrient loads and invasive *Dreissena* mussels on Lake Michigan's food web using an ecosystem model. University of Michigan, Thesis
- Bourdeau PE, Pangle KE, Peacor SD (2015) Factors affecting the vertical distribution of the zooplankton assemblage in Lake Michigan: the role of the invasive predator *Bythotrephes longimanus*. *J Great Lakes Res* 41(sp3):115–124
- Boyce FM (1974) Some aspects of Great Lakes physics of importance to biological and chemical processes. *J Fish Res Board Can* 31:689–730
- Bravo HR, Hamidi SA, Val Klump J, Waples JT (2017) Physical drivers of the circulation and thermal regime impacting seasonal hypoxia in Green Bay, Lake Michigan. In: Justic D, Rose KA, Hetland RD, Fennel K (eds) *Modeling coastal hypoxia: numerical simulations of patterns, controls and effects of dissolved oxygen dynamics*. Springer International Publishing, Cham, pp 23–47
- Bunnell DB, Carrick HJ, Madenjian CP, Rutherford ES, Vanderploeg HA, Barbiero RP, Hinchey-Malloy E, Pothoven SA, Riseng CM, Claramunt RM et al (2018) Are changes in lower trophic levels limiting prey-fish biomass and production in Lake Michigan?

- [online]. Available from: <http://www.glfsc.org/pubs/misc/2018-01.pdf> [accessed 24 May 2018]
- Cannon DJ, Troy C, Bootsma H, Liao Q, MacLellan-Hurd RA (2021) Characterizing the seasonal variability of hypolimnetic mixing in a large, deep lake. *J Geophys Res: Oceans* 126:e2021JC017533
- Cannon D, Fujisaki-Manome A, Wang J, Kessler J, Chu P (2023) Modeling changes in ice dynamics and subsurface thermal structure in Lake Michigan-Huron between 1979–2021. *Ocean Dynamics* 73:201–218. <https://doi.org/10.1007/s10236-023-01544-0>
- Chen CS, Ji RB, Schwab DJ, Beletsky D, Fahnenstiel GL, Jiang MS, Johengen TH, Vanderploeg H, Eadie B, Budd JW, Bundy MH, Gardner W, Cotner J, Lavrentyev PJ (2002) A model study of the coupled biological and physical dynamics in Lake Michigan. *Ecol Model* 152:145–168
- Chen C, Liu H, Beardsley RC (2003) An unstructured grid, finite-volume, three-dimensional, primitive equations ocean model: application to coastal ocean and estuaries. *J Atmos Oceanic Tech* 20(1):159–186
- Chen C, Beardsley R, Cowles G (2006) An unstructured grid, Finite-Volume Coastal Ocean Model (FVCOM) system. *Oceanography* 19:78–89. <https://doi.org/10.5670/oceanog.2006.92>
- Chen C, Beardsley RC, Cowles G, Qi J, Lai Z, Gao G, Stuebe D, Xu Q, Xue P, Ge J, Ji R, Hu S, Tian R, Huang H, Wu L, Lin H (2013) An unstructured-grid, finite-volume community ocean model: FVCOM user manual. Sea Grant College Program, Massachusetts Institute of Technology, Cambridge, MA, USA
- Eppehimer DE, Bunnell DB, Armenio PM, Warner DM, Eaton LA, Wells DJ, Rutherford ES (2019) Densities, diets, and growth rates of larval Alewife and Bloater in a changing Lake Michigan ecosystem. *Trans Am Fish Soc* 148:755–770
- Fahnenstiel G, Nalepa T, Pothoven S, Carrick H, Scavia D (2010) Lake Michigan lower food web: long-term observations and *Dreissena* impact. *J Great Lakes Res* 36(sp3):1–4
- Fulton EA (2001) The effects of model structure and complexity on the behavior and performance of marine ecosystem models. Dissertation, University of Tasmania, Hobart, Tasmania, Australia
- Fulton EA, Smith ADM, Johnson CR (2003) Mortality and predation in ecosystem models: is it important how these are expressed? *Ecol Model* 169:157–178
- Fulton EA, Smith ADM, Johnson CR (2004a) Biogeochemical marine ecosystem models I: IGBEM - a model of marine bay ecosystems. *Ecol Model* 174:267–307
- Fulton EA, Parslow JS, Smith ADM, Johnson CR (2004b) Biogeochemical marine ecosystem models II: the effect of physiological detail on model performance. *Ecol Model* 173:371–406
- Fulton EA, Smith ADM, Johnson CR (2004c) Effects of spatial resolution on the performance and interpretation of marine ecosystem models. *Ecol Model* 176:27–42
- Gao G, Chen C, Qi J, Beardsley RC (2011) An unstructured-grid, finite-volume sea ice model: development, validation, and application. *J Geophys Res Oceans* 116:1–15. <https://doi.org/10.1029/2010JC006688>
- Hecky RE, Smith REH, Barton DR, Guildford SJ, Taylor WD, Charlton MN, Howell T (2004) The nearshore phosphorus shunt: a consequence of ecosystem engineering by dreissenids in the Laurentian Great Lakes. *Can J Fish Aquat Sci* 61:1285–1293
- Hu H, Wang J (2010) Modeling effects of tidal and wave mixing on circulation and thermohaline structures in the Bering Sea: process studies. *J Geophys Res* 115:C01006. <https://doi.org/10.1029/2008JC005175>
- Hunke EC, Dukowicz JK (1997) An elastic–viscous–plastic model for sea ice dynamics. *J Phys Oceanogr* 27(9):1849–1867
- Kerfoot WC, Yousef F, Green SA, Budd JW, Schwab DJ, Vanderploeg HA (2010) Approaching storm: disappearing winter bloom in Lake Michigan. *J Great Lakes Res* 36(sp3):30–41
- Klump JV, Brunner SL, Grunert BK, Kaster JL, Weckerly K, Houghton EM, Kennedy JA, Valenta TJ (2018) Evidence of persistent, recurring summertime hypoxia in Green Bay, Lake Michigan. *J Great Lakes Res* 44:841–850
- Koseff JR, Hohen JK, Monismith SG, Cloern JE (1993) Coupled effects of vertical mixing and benthic grazing on phytoplankton populations in shallow, turbid estuaries. *J Mar Res* 51(4):843–868
- Krantzberg G, De Boer C (2008) A valuation of ecological services in the Laurentian Great Lakes Basin with an emphasis on Canada. *J Am Water Works Ass* 100:100–111
- Larson G, Schaeztl R (2001) Origin and evolution of the Great Lakes. *J Great Lakes Res* 27:518–546
- Leonhardt BS, Happel A, Bootsma H, Bronte CR, Czesny S, Feiner Z, Kornis MS, Rinchar J, Turschak B, Höök T (2020) Diet complexity of Lake Michigan salmonines: 2015–2016. *J Great Lakes Res* 46:1044–1057
- Li Y, Beletsky D, Wang J, Austin JA, Kessler J, Fujisaki-Manome A, Bai P (2021) Modeling a large coastal upwelling event in Lake Superior. *J Geophys Res: Oceans* 126. <https://doi.org/10.1029/2020JC016512>
- Luo L, Wang J, Hunter T, Wang D, Vanderploeg H (2017) Modeling spring–summer phytoplankton bloom in Lake Michigan with and without riverine nutrient loading. *Ocean Dyn* 67(11):1481–1494. <https://doi.org/10.1007/s10236-017-1092-x>
- Luo L, Wang J, Schwab DJ, Vanderploeg H, Leshkevich G, Bai X, Hu H, Wang D (2012) Simulating the 1998 spring bloom in Lake Michigan using a coupled physical-biological model. *J Geophys Res* 117. <https://doi.org/10.1029/2012JC008216>
- Madenjian CP, Bunnell DB, Warner DM, Pothoven SA, Fahnenstiel GL et al (2015) Changes in the Lake Michigan food web following dreissenid mussel invasions: a synthesis. *J Great Lakes Res* 41:217–231
- Madenjian CP [ed] (2019) The state of Lake Michigan in 2016. Great Lakes Fishery Commission Special Publication. [http://www.glfsc.org/pubs/SpecialPubs/Sp19\\_01.pdf](http://www.glfsc.org/pubs/SpecialPubs/Sp19_01.pdf) (accessed 12 Nov 2021)
- McMeans BC, McCann KS, Tunney TD, Fisk AT, Muir AM, Lester N, Shuter B, Rooney N (2016) The adaptive capacity of lake food webs: from individuals to ecosystems. *Ecol Monogr* 86:4–19
- McNaught DC, Hasler AD (1961) Surface schooling and feeding behavior in the white bass, *Roccus chrysops* (Rafinesque), in Lake Mendota. *Limnol Oceanogr* 6:53–60
- Miller TR, Tarpey W, Nuese J, Smith M (2022) Real-time monitoring of cyanobacterial harmful algal blooms with the Panther Buoy. *ACS ES&T Water* 2:1099–1110
- NOAA GLERL (2019a) Long-term vertical water temperature observations in the deepest area of Lake Michigan’s southern basin. NOAA National Centers for Environmental Information. Dataset. <https://www.ncei.noaa.gov/archive/accession/GLERL-LakeMI-DeepSouthernBasinWaterTemp>. Accessed 1 Feb 2022
- NOAA GLERL (2019b) Water temperature collected at multiple depths from a mooring in central Lake Huron, Great Lakes region from 2012–10–23 to 2019b-06–28 (NCEI Accession 0191817). NOAA National Centers for Environmental Information. Dataset. <https://www.ncei.noaa.gov/archive/accession/0191817>. Accessed 1 Feb 2022
- Ozersky T, Bramburger AJ, Elgin AK, Vanderploeg HA, Wang J, Austin JA et al (2021) The changing face of winter: lessons and questions from the Laurentian Great Lakes. *J Geophys Res: Biogeosci* 126:e2021JG006247
- Plattner S, Mason DM, Leshkevich GA, Schwab DJ, Rutherford ES (2006) Classifying and forecasting coastal upwellings in Lake Michigan using satellite derived temperature images and buoy data. *J Great Lakes Res* 32(1):63–76
- Pothoven SA, Vanderploeg HA (2020) Seasonal patterns for Secchi depth, chlorophyll a, total phosphorus, and nutrient limitation

- differ between nearshore and offshore in Lake Michigan. *J Great Lakes Res* 46:519–527
- Rao YR, Schwab DJ (2007) Transport and mixing between the coastal and offshore waters in the Great Lakes: a review. *J Great Lakes Res* 33(1):202–218
- Rowe MD, Obenour DR, Nalepa TF, Vanderploeg HA, Yousef F, Kerfoot WC (2015) Mapping the spatial distribution of the biomass and filter-feeding effect of invasive dreissenid mussels on the winter-spring phytoplankton bloom in Lake Michigan. *Freshw Biol* 60:2270–2285
- Rowe MD, Anderson EJ, Vanderploeg HA, Pothoven SA, Elgin AK, Wang J, Yousef F (2017) Influence of invasive quagga mussels, phosphorus loads, and climate on spatial and temporal patterns of productivity in Lake Michigan: a biophysical modeling study. *Limnol Oceanogr* 62:2629–2649
- Rutherford ES, Zhang H, Kao YC, Mason DM, Shakoo A, Bouma-Gregson K, Breck JT, Lodge DM, Chadderton WL (2021) Potential effects of bigheaded carps on four Laurentian Great Lakes food webs. *North Am J Fish Manag* 41:999–1019
- Shen C, Liao Q, Bootsma HA, Troy CD, Cannon D (2018) Regulation of plankton and nutrient dynamics by profundal quagga mussels in Lake Michigan: a one-dimensional model. *Hydrobiologia* 815(1):47–63
- Shen C, Liao Q, Bootsma HA (2020) Modelling the influence of invasive mussels on phosphorus cycling in Lake Michigan. *Ecol Model* 416:108920. <https://doi.org/10.1016/j.ecolmodel.2019.108920>
- Tellier JM, Kalejs NI, Leonhardt BS, Cannon D, Höök TO, Collingsworth PD (2022) Widespread prevalence of hypoxia and the classification of hypoxic conditions in the Laurentian Great Lakes. *J Great Lakes Res* 48:13–23
- Tomlinson LM, Auer MT, Bootsma HA, Owens EM (2010) The Great Lakes *Cladophora* model: development, testing, and application to Lake Michigan. *J Great Lakes Res* 36:287–297
- Trumpinkas J, Rennie MD, Dunlop ES (2022) Seventy years of food-web change in South Bay, Lake Huron. *J Great Lakes Res* 48:1248–1257
- Vanderploeg HA, Nalepa TF, Jude DJ, Mills EL, Holeck KT, Liebig JR, Grigorovich IA, Ojaveer H (2002) Dispersal and emerging ecological impacts of Ponto-Caspian species in the Laurentian Great Lakes. *Can J Fish Aquat Sci* 59(7):1209–1228
- Vanderploeg HA, Liebig JR, Nalepa TF, Fahnenstiel GL, Pothoven SA (2010) *Dreissena* and the disappearance of the spring phytoplankton bloom in Lake Michigan. *J Great Lakes Res* 36:50–59
- Vanderploeg HA, Pothoven SA, Krueger D, Mason DM, Liebig JR, Cavaletto JF, Ruberg SA, Lang GA, Ptáčnicková R (2015) Spatial and predatory interactions of visually preying nonindigenous zooplankton and fish in Lake Michigan during midsummer. *J Great Lakes Res* 41(sp3):125–142
- Wang J, Bai X, Hu H, Clites A, Colton M, Lofgren B (2012) Temporal and spatial variability of Great Lakes ice cover, 1973–2010. *J Clim*. <https://doi.org/10.1175/2011JCL14066.1>
- Wang J, Manome A, Kessler J, Cannon D, Chu P (2023) Inertial Instability and Phase Error in Euler Forward Predictor-Corrector Time Integration Schemes: Application to the improvement of modeling thermal structure in the Great Lakes. *Ocean Dynamics*. <https://doi.org/10.1007/s10236-023-01558-8>
- Wetzel RG (2001) *Limnology: Lake and River Ecosystems*. Academic Press, San Diego, California